Antisite disorder-induced low-field magnetoresistance in some frustrated Sr_2FeMoO_6

2006 J. Phys.: Condens. Matter 18 11347

(http://iopscience.iop.org/0953-8984/18/49/025)

INSTITUTE OF PHYSICS PUBLISHING JOURNAL OF PHYSICS: CONDENSED MATTER

J. Phys.: Condens. Matter **18** (2006) 11347–11355 doi:10.1088/0953-8984/18/49/025

Antisite disorder-induced low-field magnetoresistance in some frustrated Sr_2FeMoO_6

Tian-Yi Cai[1,2], **Sheng Ju**[1] **and Zhen-Ya Li**[1,3,4]

[1] Department of Physics, Suzhou University, Suzhou 215006, People's Republic of China
[2] Institute of Physics, Chinese Academy of Sciences, Beijing 100080, People's Republic of China
[3] CCAST (World Laboratory), PO Box 8730, Beijing 100080, People's Republic of China

E-mail: tycai@aphy.iphy.ac.cn and zyli@suda.edu.cn

Received 21 March 2006, in final form 6 September 2006
Published 23 November 2006
Online at stacks.iop.org/JPhysCM/18/11347

Abstract

Considering the existence of antiferromagnetic patches induced by the antisite disorder in ferrimagnetic Sr_2FeMoO_6, we have developed a resistor network model to account for the effects of the antisite disorder on the magnetoresistance in this material. It is proposed that the magnetic disorder resulting from the existence of frustration around the antiferromagnetic patches will be suppressed under the applied magnetic field and low-field magnetoresistance will be observed. For samples with low levels of antisite defects, the magnetoresistive behaviour may be strongly affected by the different degrees of magnetic inhomogeneity. Our calculated results are in agreement with experimental observations.

1. Introduction

Recently, the double perovskite Sr_2FeMoO_6 (SFMO) has attracted considerable attention because of the significant magnetoresistance (MR) at 300 K under a magnetic field $H < 2$ kOe [1], which has not been observed in the perovskite manganites. The experimental results of the optical conductivity spectrum indicate that Sr_2FeMoO_6 has a half-metallic electronic structure [2]. Band structure calculations show that the majority spin band is gapped and the corresponding $3d^5$ spin-up electrons localize in the Fe^{3+} ions while the conduction band is partially occupied by the $4d^1$ spin-down electrons of Mo^{5+} ions. A large antiferromagnetic superexchange interaction between the $S = 5/2$ spins of Fe^{3+} and the $S = 1/2$ spins of Mo^{5+} induces a ferrimagnetic half-metallic state with a large saturation moment of $4\mu_B$. The observed magnetic transition temperature is as high as 410–450 K [3, 4]. Due to its high ferromagnetic transition temperature and half-metallic structure, the unusually high spin polarization of conduction electrons (>60%) can persist even around room temperature (RT). These properties may lead to the large low-field magnetoresistance (LFMR) at RT. As a result,

[4] Address for correspondence: Department of Physics, Suzhou University, Suzhou 215006, People's Republic of China.

0953-8984/06/4911347+09$30.00

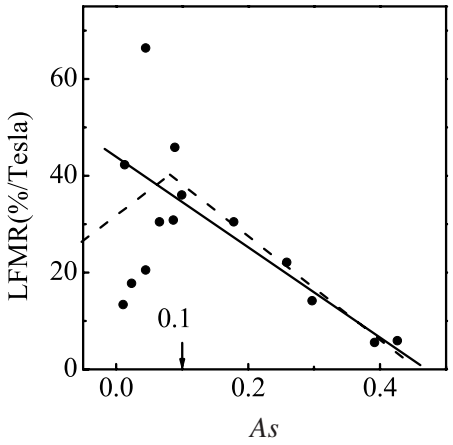

Figure 1. Reported data concerning the evolution of the LFMR with the Fe/Mo antisite disorder per formula unit ($0 < As \leqslant 0.5$) in polycrystalline Sr_2FeMoO_6 materials [9, 10]. The solid line shows the *As* dependence of the MR, reproduced from [9]. The dashed line shows the relation between *As* and MR proposed in [11].

Sr_2FeMoO_6 could be proposed as a better candidate material to be used in spintronics than other half-metallic materials.

Two alternative origins of the LFMR in Sr_2FeMoO_6 have been proposed in the previous studies. In one view, like the LFMR observed in doped manganites, the LFMR of Sr_2FeMoO_6 polycrystalline samples is attributed to the spin-dependent transfer of electrons across grain boundaries (GBs). It is therefore possible to enhance the LFMR by modifying the GBs of this compound, such as by reducing the grain size [5], using the grain boundary of a bicrystal [6], and even changing the properties of grain surfaces by controlling the oxygen content [7, 8]. Although most studies suggest that the grain boundaries are responsible for the LFMR in SFMO, there are also reports suggesting that the LFMR is connected to the *antisite disorder*, where some of the Fe and Mo ions interchange their crystallographic positions. García-Hernández *et al* [9] examine several compounds of the series $A_{2-x}A'_xFeMoO_6$, in which A is an alkaline earth atom and A′ is an aliovalent cation such as La. They find that where there is a moderate level of antisite disorder at the Fe and Mo sites, antiferromagnetic Fe–O–Fe patches naturally develop in the material and the LFMR results from the spin-dependent transmissivity of the antisite-disordered patches. Furthermore, they observe that the magnitude of the LFMR decreases almost linearly with the increase of disorder. However, when the concentration *As* of antisite disorder is less than 0.1, different samples show inconsistent LFMR behaviours. On the other hand, Navarro *et al* [10] claim that for the samples of $As < 0.09$, the MR increases with an increase in antisite disorder. In their studies, polycrystalline SFMO samples having higher antisite disorder show larger MR than those with less disorder. Recently, Sánchez *et al* [11] have characterized the antisite disorder-induced MR, which arises from a moderate concentration of antisite defects and vanishes for massive *As* levels. These experimental results have been illustrated in figure 1.

These controversial experimental results (figure 1) show that the role of the antisite disorder on the LFMR response has not been explored enough and remains unclear. The dependence of LFMR on *As* is still a puzzling fact. It has been shown that there is a close connection between the concentration of antisite defects and the difficulty to magnetically saturate the material, which can be easily understood if antisite defects are the source of a

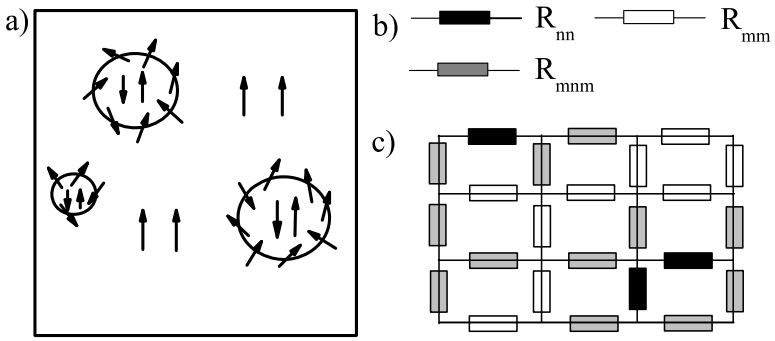

Figure 2. An example of the construction of an RRN. (a) Schematic picture of the Sr_2FeMoO_6 samples with antisite disorder. (b) Three types of scattering resistor due to different interfaces: R_{nn}, R_{mm} and R_{mnm}. (c) The constructed random resistor network given a certain ratio of different resistors, which is closely related to As.

significant magnetic frustration [10, 11]. In this paper, considering the existence of magnetic frustration around the antisite defects, we have studied the magnetic transport properties in single-crystalline Sr_2FeMoO_6 samples to examine antisite disorder-induced MR behaviours. The dependence of LFMR on As is obtained and analysed explicitly.

2. Model

We propose the following model to explain the observed LFMR as a direct consequence of the antisite disorder. In ordered Sr_2FeMoO_6, the alternating ordering of Fe and Mo is fulfilled. Whereas the Fe–Mo–Fe neighbours couple ferrimagnetically, the Fe–Fe correlations at the antisites are antiferromagnetic [12]. Consequently, antisite disorder implies the existence of Fe–O–Fe antiferromagnetic (AF) patches across a sample in between the ordered ferromagnetic (FM) volumes. The existence of the AF patches has been firmly established by Mössbauer spectroscopy and is related to the high-spin component Fe^{3+} while a fluctuating valence state $Fe^{2.5+}$ would correspond to the perfectly ordered volumes [13]. For small antisite disorder, the Fe–O–Fe patches are not very large; the AF interaction has to compete with the FM ones imposed by the surrounding material. This, in turn, generates an important frustration primarily localized in the surroundings of the AF antisite patches [14] as illustrated in figure 2(a), in agreement with what is observed in hysteresis cycles. The AF Fe–O–Fe patches and the generated frustrated layers act as barriers to the electronic transport between the ordered volumes [9]. When As is small, the AF patches may be considered as islands embedded in a ferromagnetic (FM) matrix and the interfaces between these two phases are magnetically frustrated regions. Consequently, the epitaxial film of Sr_2FeMoO_6 may be assumed to be composed of FM matrix (ordered volumes), AF patches and magnetically frustrated interfaces (antisite defects). The conduction may be modelled by considering three different types of resistor based on the different scattering processes (shown in figure 2(b)). (1) R_{nn} represents the scattering processes within AF patches. (2) R_{mm} models the scattering processes within the perfect ordered volume. (3) R_{mnm} models the scattering from an ordered region to a neighbouring ordered region through the frustrated interfaces when the separation between the two ordered regions is smaller than the electronic mean free path (mfp) λ (in our model, the case that the separation is larger than λ is not considered due to the weak magnetic field dependence). Within this scenario, the electron scattering processes can be mapped onto a

random resistor network (RRN) with different kinds of resistor. The RRN was defined on a cubic or square lattice, but with a lattice spacing much larger than the several angstroms distance between nearest-neighbour ions. Actually, the random network does not mimic the complicated distribution of antisite disorder, but tries to show the contributions of different interfaces to scattering resistances. A schematic representation is presented in figure 2(c).

Interface scattering dominates the spin-dependent processes in the Sr_2FeMoO_6 samples with antisite disorder, since a perfect Sr_2FeMoO_6 crystal is expected to show no MR effects at temperatures far below T_C [4]. Consequently, R_{nn} and R_{mm} may be spin independent and taken as constants R_1 and R_2, while R_{mnm} is spin dependent. For the scattering of a electron from the ith ordered region to the jth region through the frustrated interfaces, the spin-dependent part of resistance R_{mnm} is related to the angle θ_{ij} between the magnetic moments μ_i and μ_j. The resistance will be low (high) when μ_i and μ_j are parallel (antiparallel). R_{mnm} can be written as $R_{mnm} = R_0 - PR_S \cos\theta_{ij}^{(\lambda)}$, where R_0 and R_S are constants describing the spin-independent and spin-dependent components of the interface resistance. P denotes the spin polarization.

For a given concentration of antisite disorder, temperature, and applied field, the earlier expressions should be averaged over different configurations of the magnetic moments. The statistically averaged resistances take on the forms

$$R'_{nn} = R_{nn} = R_1 \tag{1}$$

$$R'_{mm} = R_{mm} = R_2 \tag{2}$$

$$R'_{mnm} = R_0 - \alpha \left\langle \cos\theta_{ij} \right\rangle_\lambda . \tag{3}$$

$\langle \cdots \rangle$ means the average to be performed over all (i, j) pairs whose distance r_{ij} is of the order of magnitude of the electron mfp λ. The constant α in equation (3) is used to substitute PR_S. Using straightforward trigonometric relations, and factorizing the averages over colatitude and azimuth, one gets

$$\langle \cos\theta_{ij} \rangle = \langle \cos\theta_i \cos\theta_j \rangle + \langle \sin\theta_i \sin\theta_j \rangle \times \langle \cos(\phi_i - \phi_j) \rangle. \tag{4}$$

For assumed random anisotropy and non-interacting particles, the hypothesis of lack of correlation between tilt and twist angles of any pair of magnetic moments is made; as a consequence, $\langle \cos\theta_{ij} \rangle = \langle \cos\theta_i \cos\theta_j \rangle = (M/M_S)^2$. This is true in paramagnetic systems owing to the dominant thermal effects acting on each moment. In the present case, the local canting of magnetic moments is determined by the competition between magnetic interactions. Therefore, the couplings between moments in ordered FM volumes should be considered.

In order to phenomenologically describe the FM correlation in ordered volumes, this correlation is assumed to monotonically decrease with increasing r_{ij} [15, 16], and we obtain

$$\langle \cos(\phi_i - \phi_j) \rangle = \mathrm{e}^{(-r_{ij}/r_m)} \tag{5}$$

$$\langle \cos\theta_i \cos\theta_j \rangle = \langle \cos\theta \rangle^2 + (\langle \cos^2\theta \rangle - \langle \cos\theta \rangle^2)\mathrm{e}^{(-r_{ij}/r_m)} \tag{6}$$

$$\langle \sin\theta_i \sin\theta_j \rangle = \langle \sin^2\theta \rangle \mathrm{e}^{(-r_{ij}/r_m)} \tag{7}$$

where r_m is the correlation range. Equation (4) turns out to be

$$\langle \cos\theta_{ij} \rangle = \langle u \rangle^2 + (\langle u^2 \rangle - \langle u \rangle^2)\mathrm{e}^{-r_{ij}/r_m} + (1 - \langle u^2 \rangle)\mathrm{e}^{-2r_{ij}/r_m} \tag{8}$$

where $\langle u \rangle$ corresponds to the reduced magnetization M/M_S. To obtain the quantity $\langle u^2 \rangle$, a simplified picture of the magnetization mechanism in frustrated magnets may be used [16]. It is supposed here that the distribution at equilibrium of the local directions of the magnetization under a given magnetic field may be represented by the spherical random-walk function introduced by Zener [17]. The relationship between $\langle u^2 \rangle$ and $\langle u \rangle$ is easily obtained by exploiting the orthogonality of Legendre polynomials; as it turns out,

$$\langle u^2 \rangle = \tfrac{1}{3} + \tfrac{2}{3}\langle u \rangle^3. \tag{9}$$

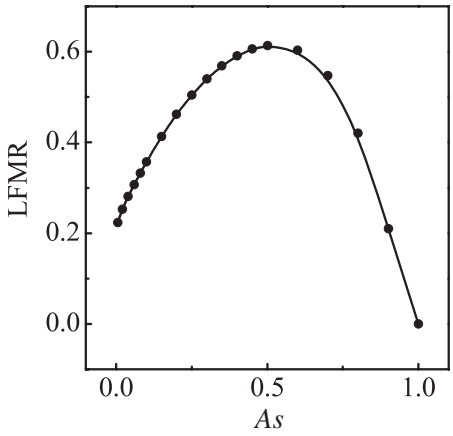

Figure 3. The dependence of the magnetoresistance on the concentration of the antisite disorder without considering the effect of the frustration.

Combined with equations (3), (8) and (9), R'_{mnm} may be represented as

$$R'_{mnm} = R_0 - \alpha[\langle u\rangle^2 + (\tfrac{2}{3}\langle u\rangle^3 - \langle u\rangle^2 + \tfrac{1}{3})e^{-\lambda/r_m} - (\tfrac{2}{3}\langle u\rangle^3 - \tfrac{2}{3})e^{-2\lambda/r_m}], \tag{10}$$

where the condition $r_{ij} = \lambda$ is introduced.

Our constructed RRN includes three types of conductor with conductances G_i $(=1/R_i)$ and concentrations p_i $(i = 1\text{–}3)$. In perfect ordered Sr_2FeMoO_6, the ideal saturation magnetization is $4\mu_B$. Antisite disorder, i.e., misoccupancy of the Fe and Mo sublattices, will lower the expected saturation magnetization of $4\mu_B$ by inducing Fe–O–Fe antiferromagnetic (AF) patches. Assuming the random distribution of antisite disorder and from the viewpoint of mean-field theory, the volume fraction f of AF patches may be determined by $(1 - M_S/4\mu_B)$, where M_S is the saturated magnetization of the samples with antisite disorder $(M_S < 4\mu_B)$. Furthermore, f may be related to As mediated by the previous theoretically prediction $M_S = (3.53\text{–}3.6 \times As)\mu_B$ [18], which agrees well with the experimental results [9]. In our calculations, we take f^2 to be the concentration of R_{nn}-type resistors and $(1 - f)^2$ to be that of the R_{mm}-type resistors. The R_{mnm}-type resistors make up the remaining concentration of $2f(1 - f)$. The effective conductance can be calculated using the effective medium approximation (EMA) method [19, 20],

$$\sum_{i=1}^{3} p_i \frac{G_i - G_e}{G_i + 2G_e} = 0. \tag{11}$$

The magnetoresistance can be calculated via

$$\mathrm{MR} = \frac{G_e(DM) - G_e(M)}{G_e(M)}, \tag{12}$$

where $G_e(DM)$ and $G_e(M)$ represent the effective conductance at the demagnetized and magnetic states, respectively.

3. Results and discussions

The intuitive influence of magnetic disorder around the antisites may be the reduction of mean free path (mfp) λ. Figure 3 gives the calculated results where the mfp is kept constant with the increasing As. It is shown that the maximum of the LFMR locates around $As = 0.5$, which

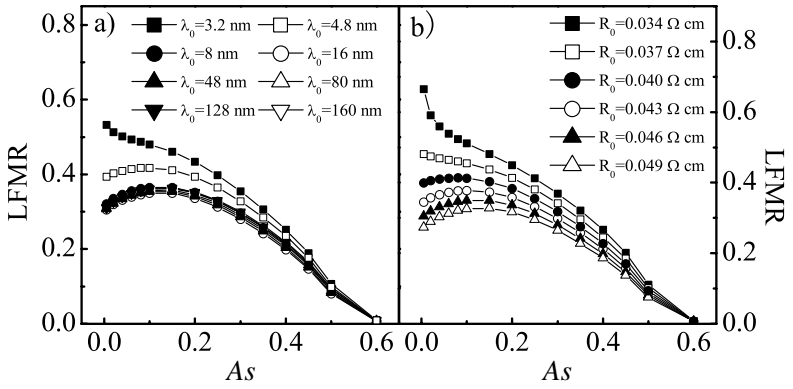

Figure 4. (a) As-dependent MR with different λ_0 (R_0 is fixed at 4.6×10^{-2} Ω cm). (b) As-dependent MR with different R_0 (λ_0 is fixed as 16 nm).

is not in agreement with the experimental results (the maximum of the LFMR is often around $As = 0.1$). These results indicate that the role of the magnetically frustrated interface induced by antisite defects on the LFMR could not be neglected.

To quantitatively demonstrate the effect of frustration on the LFMR, a linear decay of λ with As is assumed:

$$\lambda = \lambda_0(1 - As), \tag{13}$$

which is the simplest formula to describe the effect of antisite disorder on λ. Ordered samples ($As = 0.0$) have the maximum value of electronic mfp λ_0. In contrast, the mfp λ may approach zero for completely disordered samples ($As = 1.0$). Here the ultra-short-range magnetic inhomogeneity comes from the magnetic frustration effect originated by competing interactions. It is difficult to provide an accurate theoretical description of the equilibrium spin arrangement, as well as an experimentally measured value of the electron mfp. Therefore, λ_0 is assumed to be varied (3.2–160 nm) according to most disordered metallic alloys with an electronic mfp of the order of a few nanometres [16]. As shown in equation (10), by effect of the competition with spin correlation length r_m, λ gives an important contribution to the spin-dependent resistance. In this sense, the parameter r_m/λ should be paid more attention to than r_m or λ. In our calculations, the correlation length r_m is assumed to be 2 and 100 nm at the demagnetized and magnetic states, respectively. This leads to r_m/λ varying with the ranges of 10^1–10^{-2} and 10^2–10^{-1} at the demagnetized and magnetic states, respectively. The ordered SFMO samples have long been known as conductors [22], so R_2 is assumed to be a constant, 10^{-4} Ω cm. Although $SrFe^{4+}O_3$ has a metallic conductivity, the increase of Fe^{3+} by introduction of oxygen deficiencies will lead to an insulating phase with a resistivity (R_1) of about 10^{-1} Ω cm [23]. As discussed above, the correlation length λ/r_m must vanish for high fields. As a consequence, the electrical resistance R_{mnm} must depend on the square of the reduced magnetization for sufficiently high values of the magnetic field: $R_{mnm} = R_0 - \alpha\langle u\rangle$ [2]. For samples with $As \approx 0.1$, R_{mnm}-type resistors dominate the electric transport (this will be explained in the following text). By fitting the experimental data for $As = 0.13$ [2], R_0 and α are chosen to be 4.6×10^{-2} Ω cm and 3×10^{-3} Ω cm, respectively. Figure 4(a) shows the MR curves as a function of As with different λ_0 values. It is interesting that the maximum attainable LFMR ratio is around $As = 0.1$ for high λ_0 values ($\lambda_0 > 4.8$ nm), while for small λ_0 values (i.e., $\lambda_0 = 3.2$ nm), the LFMR decreases monotonically over the entire As range. In figure 4(b) the LFMR is given as a function of As (for a constant λ_0 and various R_0 values). It

is found that for the large R_0 ($R_0 \geqslant 4.0 \times 10^{-2}$ Ω cm) the MR plots peak around $As = 0.1$ and the peaks will shift to the low-As regime with the decrease of R_0. In contrast, for small R_0 ($R_0 \leqslant 3.7 \times 10^{-2}$ Ω cm) the decreases of LFMR with increasing As are observed. Furthermore, when As is very close to zero, the samples with smaller R_0 will have a higher LFMR.

Calculated results show that the complicated LFMR behaviours for the samples with $As < 0.1$ observed experimentally may be related to the intrinsic ultra-short-range magnetic inhomogeneity coming from magnetic frustration. Due to different synthesis routes or annealing steps, although the SFMO samples have the same level of antisite disorder, the morphologies (i.e., the distribution of antisite defects, the average size, the shape, and the distribution of AF patches) may be different. Therefore, the magnetic interaction between Fe ions may be different [21], as well as average degrees of magnetic frustration. As shown in figures 4(a) and (b), given the same contribution of spin-independent resistance, for large R_0 or λ_0 values, the LFMR–As curves exhibit peaks around $As = 0.1$, while for the samples with small R_0 or λ_0 the peaks disappear and the LFMR decreases monotonically. Furthermore, it is surprising why different degrees of magnetic inhomogeneity have a large effect on the MR behaviours only for $As < 0.1$. Therefore, since $As \approx 0.1$ is a critical point (the samples with $0 < As < 0.1$ may show different LFMR behaviours, i.e. $\mathrm{dLFMR}/\mathrm{d}As > 0$ or $\mathrm{dLFMR}/\mathrm{d}As < 0$), the magnetoresistive behaviours of the samples with $As \approx 0.1$ are discussed in detail. All the resistors in the RRN can be divided into spin-dependent resistors R_{mnm} and spin-independent resistors including R_{mm} and R_{nn}. $As \approx 0.1$, namely $f \approx 0.2$, implied that the concentration of R_{mnm}-type resistors is about 0.32. This is very close to the theoretical predicted percolation threshold of two-phase effective medium theory in the three-dimensional percolation model. This suggests the MR may have its maximum provided that R_{mnm}-type resistors connect and a spanning path across the sample appears with the increasing As. The observed peak in the MR curves refers to such concentration of antisite disorder in which the random configurations have an optimal number of resistors of the R_{mnm} type.

Finally, we wish to point out other issues relevant to our model. First, in previous studies, the spin polarization P is expected to decrease with As and the role of P on the antisite disorder-induced LFMR is thought to be important. However, our calculated results show that it may be insufficient to only use such a mechanism to explain the complicated LFMR behaviour. Figure 5 shows the As-dependent LFMR for decreasing α ($\propto P$). The positions of the maximum LFMR as well as the shape of LFMR–As curves are invariant, indicating the minor contribution of P to the magnetoresistive behaviours. On the other hand, as shown in figures 6(a) and (b) similar As-dependent LFMR has also been observed when λ is assumed to decrease with As in exponential forms ($\lambda = \lambda_0 \mathrm{e}^{-bAs}$), where b characterizes the attenuation velocity of λ. For comparison, all the dependences of λ on As discussed in this article are shown in figure 6(c). For small As, λ decreases more rapidly in the exponential form than in the linear one. In figure 6(d), we present the effect of parameter b on the MR–As curves. The larger b, which means more rapid decease of λ with increasing As, will give rise to more abrupt peak of MR curves. Meanwhile, the position of the peak will move to the low-As regime. But the variation of b will not change the shape of the MR curves.

4. Conclusions

In summary, the controversial LFMR behaviours induced by antisite disorder could be understood easily using intrinsic magnetic inhomogeneity. Within this scenario, the existence of antisite disorder in SFMO gives rise to the appearance of AF patches. The AF interaction within these patches has to compete with the FM ones imposed by the surrounding ordered volumes, which generates the magnetically frustrated areas separating the AF phases from

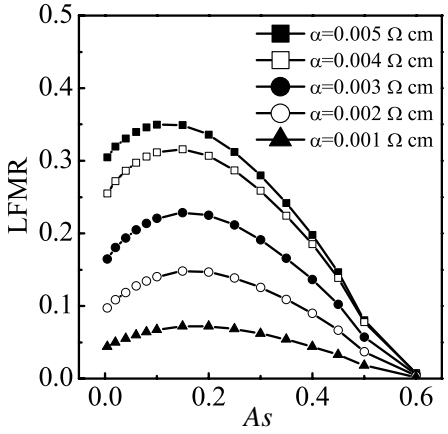

Figure 5. *As* versus MR curves for different α. In this case, λ decreases linearly with *As* and $\lambda_0 = 16$ nm, $R_0 = 4.6 \times 10^{-2}$ Ω cm.

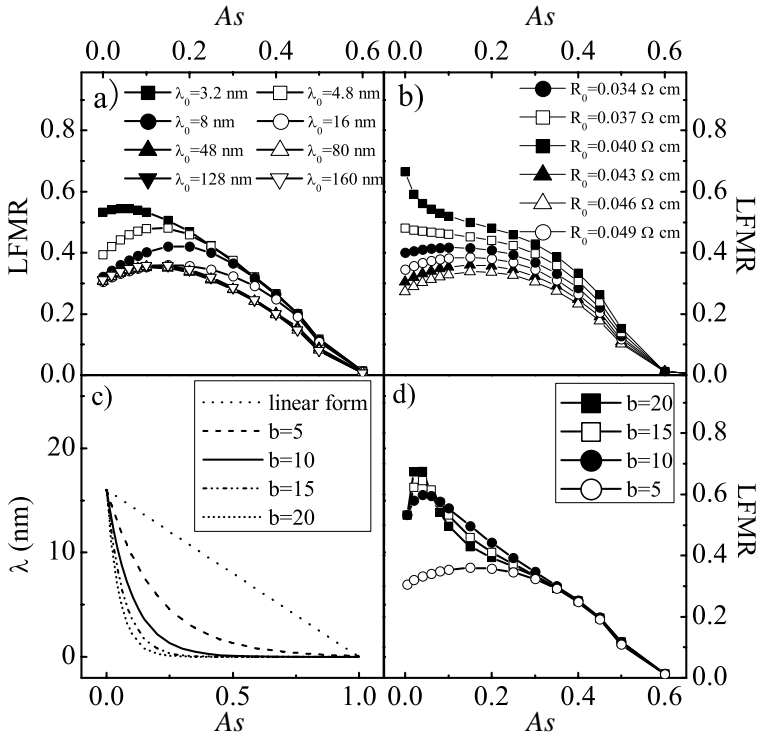

Figure 6. (a) *As* versus MR curves with different λ_0 ($R_0 = 4.6 \times 10^{-2}$ Ω cm). (b) *As* versus MR curves for different R_0 ($\lambda_0 = 16$ nm). (c) The variations of λ with *As* discussed in this paper. (d) MR as a function of *As* with different *b*.

the FM matrix. In these frustrated areas, the spin disorder supplies the extra contribution to the reduction of electronic mean free path λ. A moderate applied magnetic field suppresses the spin disorder in the magnetically frustrated areas around the antisites. This alignment of

frustrated spins promotes an effective increase of the available volume free from magnetic scattering processes. Thus, a decrease in the resistance is obtained. Although the levels of antisite disorder are the same in some samples, the properties of AF patches and magnetic frustrated area may be different since the distribution of the antisite defects may be complex and the AF patches may involve many length scales. To describe the different average degree of magnetic frustration, different values of R_0 and λ are assumed. The different degrees of magnetic frustration lead to the complex magnetoresistive behaviours of the samples with low levels of antisite disorder ($As < 0.1$). For large R_0 or λ, a peak appears in the MR–As curves as shown in figure 1 (the dashed line). For small R_0 or λ, an almost linear variation of MR with As can be observed (see the solid line in figure 1). Subsequently, the MR will have a complex LFMR behaviour for $As < 0.1$ as shown in figure 1 (the solid dots). Our calculations are in good agreement with the experimental results.

Acknowledgments

The authors gratefully acknowledge support from the National Natural Science Foundation of China under Grant Nos 10447126, 10474069, 10504023, and the Creative Program for Graduate Students of Jiangsu province, China.

References

[1] Zhou J P, Dass R, Yin H Q, Zhou J S, Rabenberg L and Goodenough J B 2000 *J. Appl. Phys.* **87** 5037
[2] Kobayashi K-I, Kimura T, Sawada H, Terakura K and Tokura Y 1998 *Nature* **395** 677
[3] Yin H Q, Zhou J S, Zhou J P, Dass R, McDevitt J T and Goodenough J B 1999 *Appl. Phys. Lett.* **18** 2812
[4] Tomioka Y, Okuda T, Okimito Y, Kumai R and Kobayashi K-I 2000 *Phys. Rev.* B **61** 422
[5] Yuan C L, Wang S G, Song W H, Yu T, Dai J M, Ye S L and Sun Y P 1999 *Appl. Phys. Lett.* **75** 3853
Yuan C L, Zhu Y and Ong P P 2003 *Appl. Phys. Lett.* **82** 934
[6] Yin H Q, Zhou J-S, Zhou J-P, Dass R, McDevitt J T and Goodenough J B 1999 *Appl. Phys. Lett.* **75** 2812
[7] Niebiekikwiat D, Caneiro A, Sánchez R D and Fontcuberta J 2001 *Phys. Rev.* B **64** 180406
[8] Sharma A, Berenov A, Rager J, Branford W, Bugoslavsky Y, Cohen L F and MacManus-Driscoll J L 2003 *Appl. Phys. Lett.* **83** 2384
[9] García-Hernández M, Martínez J L, Martínez-Lope M J, Casais M T and Alonso J A 2001 *Phys. Rev. Lett.* **86** 2443
[10] Navarro J, Balcells Ll, Sandiumenge F, Bibes M, Roig A, Martínez B and Fontcuberta J 2001 *J. Phys.: Condens. Matter* **13** 8481
[11] Sánchez D, García-Hernández M, Auth N and Jakob G 2004 *J. Appl. Phys.* **96** 2736
[12] Sánchez D, Alonso J A, García-Hernández M, Martínez-Lope M J, Martínez J L and Mellergård A 2002 *Phys. Rev.* B **65** 104426
[13] Linden J, Yamamoto T, Karppinen M and Yamauchi H 2000 *Appl. Phys. Lett.* **76** 2925
[14] Ogale A, Ogale S, Ramesh R and Venkatesan T 1999 *Appl. Phys. Lett.* **75** 537
[15] Allia P, Knobel M, Tiberto P and Vinai F 1998 *Phys. Rev.* B **52** 15398
Allia P, Tiberto P and Vinai F 1997 *J. Appl. Phys.* **81** 4599
[16] Allia P, Coisson M, Moya J, Selvaggini V, Tiberto P and Vinai F 2003 *Phys. Rev.* B **67** 174412
[17] Zener C 1954 *Phys. Rev.* **96** 1335
[18] Cai T-Y and Li Z-Y 2004 *J. Phys.: Condens. Matter* **16** 3737
[19] Kirkpatrick S 1973 *Rev. Mod. Phys.* **45** 574
[20] Ju S and Li Z Y 2004 *J. Appl. Phys.* **95** 3093
[21] Solovyev I V 2002 *Phys. Rev.* B **65** 144446
[22] Shinde S R, Ogale S B, Greene R L, Venkatesan T, Tsoi K, Cheong S W and Millis A J 2003 *J. Appl. Phys.* **93** 1605
[23] Srinath S, Mahesh Kumar M, Post M L and Srikanth H 2005 *Phys. Rev.* B **72** 054425